Development and Evaluation of a Lumbar Assisted Exoskeleton With Mixed Lifting Tasks by Various Postures

Jinke Li, Yong He, Jianquan Sun, Feng Li, Jing Ye, Gong Chen, Jianxin Pang, *Member, IEEE*, and Xinyu Wu, *Senior Member, IEEE*

***Abstract*— A large number of the WRLSs (wearable robots lumbar support) research have been presented for working efficient increase and injure risk reduction in recent years. However, the previous research can only complete the sagittal-plane lifting task, which can not adapt to the mixed lifting tasks in the actual work scene. Therefore, we presented a novel lumbar assisted exoskeleton with mixed lifting tasks by various postures based on position control, which can not only carry out the lifting tasks of sagittal-plane, but also complete the lifting tasks of sides. First, we proposed a new generation method of raising reference curves that can generate assistance curve for each user with each task, which is very convenient in mixed lifting tasks. Then, an adaptive predictive controller was designed to track the reference curves of different users under different loads, the maximum tracking errors of the angles are 2.2° and 3.3° respectively at 5kg and 15kg, and all the errors are within 3%. Compared to the condition of no exoskeleton, the average RMS (root mean square) of EMG (electromyography) for six muscles are reduced by 10.33 ± 1.44%, 9.62 ± 0.69%, 10.97 ± 0.81% and 14.48 ± 2.11% by lifting loads with stoop, squat, left-asymmetric and right-asymmetric respectively. The results demonstrate that our lumbar assisted exoskeleton presents outperformance in mixed lifting tasks by various postures.**

***Index Terms*— Exoskeleton, mixed lifting tasks, non-sagittal plane, various postures.**

Manuscript received 10 August 2022; revised 21 March 2023 and 16 April 2023; accepted 17 April 2023. Date of publication 20 April 2023; date of current version 27 April 2023. This work was supported in part by the National Natural Science Foundation of China under Grant 62125307, Grant U2013209, and Grant U2013212; in part by the NSFC-Shenzhen Robotics Research Center Project under Grant U2013207; and in part by the Shenzhen Fundamental Research Program under Grant JCYJ20220818101416035. *(Corresponding author: Xinyu Wu.)*

This work involved human subjects or animals in its research. Approval of all ethical and experimental procedures and protocols was granted by the Medical Ethics Committee of Shenzhen Institute of Advanced Technology under Application No. SIAT-IRB-200715-H0512.

Jinke Li is with the Guangdong Provincial Key Laboratory of Robotics and Intelligent System, Shenzhen Institute of Advanced Technology, Chinese Academy of Sciences, Shenzhen 518055, China, also with the SIAT Branch, Shenzhen Institute of Artificial Intelligence and Robotics for Society, Chinese Academy of Sciences, Shenzhen 518055, China, and also with the Shenzhen College of Advanced Technology, University of Chinese Academy of Sciences, Shenzhen 518055, China (e-mail: jk.li@siat.ac.cn).

Yong He, Jianquan Sun, Feng Li, and Xinyu Wu are with the Guangdong Provincial Key Laboratory of Robotics and Intelligent System, Shenzhen Institute of Advanced Technology, Chinese Academy of Sciences, Shenzhen 518055, China, and also with the SIAT Branch, Shenzhen Institute of Artificial Intelligence and Robotics for Society, Chinese Academy of Sciences, Shenzhen 518055, China (e-mail: yong.he@siat.ac.cn; jq.sun@siat.ac.cn; feng.li@siat.ac.cn; xy.wu@siat.ac.cn).

Jing Ye and Gong Chen are with the MileBot Robotics Company Ltd., Shenzhen 518055, China (e-mail: ye@milebot.com.cn; gong118911@126.com).

Jianxin Pang is with UBTECH Robotics Inc., Shenzhen 518055, China (e-mail: walton@ubtrobot.com).

Digital Object Identifier 10.1109/TNSRE.2023.3268657

I. Introduction

AT PRESENT, there are a large number of robots in factories and daily life to help people improve efficiency and reduce work damage. However, in some fields, such as transportation and airport lifting, there are still a large number of manual handling by workers due to limited working environment and other reasons. In the lifting tasks, the extension torque of the worker's torso will produce a compressive force on his/her lumbar intervertebral disc. When this pressure exceeds its strength, tissue damage may occur, which may lead to the degenerative process of intervertebral disc and eventually lead to low back pain. Therefore, compressive force is used to estimate the risk of back injury [1]. Occupational back injuries require workers to take leave to recover, so this translates into economic losses, including medical costs. Therefore, a large number of the WRLSs (wearable robots lumbar support) research have been produced in recent years [2], [3]. The WRLSs typically support the user's trunk movements during manual lifting [4], [5]. The auxiliary torque provided by WRLSs can not only reduce the muscle strength of the user's waist, but also reduce the risk of back injury. WRLSs are usually divided into two types according to whether there is power or not, passive and active.

Passive WRLSs [6], [7] generally adopt elastic devices to assist according to stretching and contraction. Maja et al. [8] proposed a reconfigurable trunk exoskeleton during different activities, this study examined how varying a trunk exoskeleton's thoracic and abdominal compression affects trunk kinematics and muscle demand during several activities. Lamers et al. [9] proposed a dual-mode back-assist exosuit with extension mechanism, the extensible exosuit could provide the low back assistance torque and reduce device-to-body forces by 36% on the shoulders and legs. Moon et al. [10] proposed a lower-back exoskeleton with a four-bar linkage

structure for powering extensor moment and lumbar traction force, this exoskeleton provided lumbar traction force, which direction is opposite to the lower back compression force, during the dynamic lifting phase, the mean and peak EMG (electromyography) of ESI (erector spinae iliocostalis) were significantly reduced by 21.0% and 18.3%. Passive WELSs have the advantage of portability. However, due to the limitation of structure, they can only carry out sagittal-plane lifting tasks, but can not complete non-sagittal lifting tasks, such as left-asymmetric and right-asymmetric.

Different from passive WRLSs, active WRLSs [11], [12] contain actuator units, so they can generally provide greater assistance. There are two main control modes of active WRLSs, torque control and position control. In terms of torque control, Lanotte et al. [13] designed an underactuated multi-joint exoskeleton for lifting applications, the single actuation unit based on a series-elastic actuation architecture could drive three output joints, which are the left and right hips and the trunk. It applied constant torque to control the exoskeleton. Poliero et al. [14] presented an active back-support exoskeleton to carrying activities, which also used constant torques to assist during lifting, the back muscles was up to 12% reduction in overall lumbar activity. Hyun et al. [15] designed an active waist assisted exoskeleton H-WEXv2, which utilized a wire-driven mechanism based on a singular series elastic actuation,it could assist in semi-squat and stoop, and the muscle intensity of erector spinae and gluteus maximus was reduced by 40.7% and 41.1 % respectively in stoop posture, and 33.0% and 41.6% respectively in semi-squat posture. However, when generating the assisted torque, it needed to set the mass of carrying heavy objects, which is very inconvenient in large-scale applications.

In terms of position control, Wei et al. [16] proposed a hip active assisted exoskeleton, it obtained the reference assisted curve by the average height and weight distribution of the adult male body, so it was fixed and only assisted the squat lifting, the EMG signal of the vertical spine at L5/S1 was reduced by 30–48%, and the metabolic cost of energy was reduced by 18% compared the situation of without EXO. Seong et al. [17] developed a twisted string actuator-based exoskeleton for hip joint assistance in stoop lifting task, it obtained the reference assisted by the motion capture system during lifting of a 10-kg object. However, it can be only capable of generating required torque and speed at the hip joint while weighing under 6 kg. Chen et al. [18] designed a real-time two-step algorithm for a portable hip exoskeleton. Only using the exoskeleton-embedded sensors, they can detect the onset of the lifting movement and classify the technique used to accomplish the lift. But they did not give the control method in various cases. Xia et al. [19] used the quintic polynomial to generate the reference curve for repeat squat lifting, and used iterative learning to track the curve, this algorithm combined with the exoskeleton could reduce the strain of the user's lumbar over 40% when they lift heavy objects. However, the assisted curve was fixed for everyone and the iterative learning method failed when multiple lifting tasks are mixed.

To sum up, most WRLSs with torque control mode adopt constant torque value. WRLSs with position control usually use fixed reference curves, which can not generate personalized reference assisted curves for different people. And all the above WRLSs can only assist in the sagittal-plane. Therefore, this work designs an active lumbar assisted exoskeleton with various lifting tasks by position control mode. The major contributions of this work are as follows:

1) A new generation method of raising reference curve is proposed, which can generate assistance curve for each user with mixed lifting tasks by various postures, such as squat, stoop, left-asymmetric and right-asymmetric.
2) An adaptive predictive controller is designed, which could track the reference curves of different users under different loads.
3) The effects of curve tracking and assistance efficiency are evaluated. The tracking performance of the controller to the reference curve and the assistance effect of the assisted exoskeleton are verified.

The remainder of this work is organized as follows: Section II describes the raising reference curve generator and the design of controller in detail. Section III presents the evaluation and experimental results. In Section IV, the discussion of this work is elaborated, and the conclusion is presented in Section V.

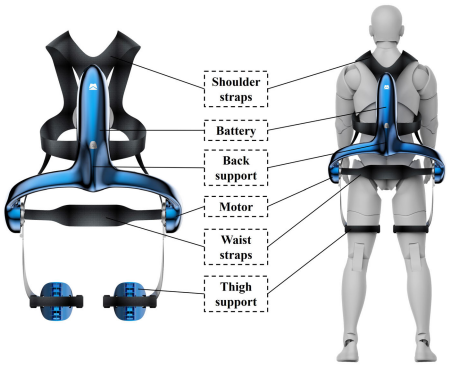

Fig. 1. The overall scheme of the lumbar assisted exoskeleton.

II. Design of Controller

A. System Overview

As shown in Fig. 1, the active assisted exoskeleton is designed. The whole mass of this exoskeleton is 6kg, and most of the weight is concentrated at the waist. This is the position of the user's center of gravity, which can minimize the impact on the user's natural movement.

The structure of this exoskeleton is mainly composed of six parts. The back support and binding structure fit with the human waist, which are the main structure of the lumbar exoskeleton; Back support, thigh support, shoulder straps and waist straps evenly distribute the auxiliary torque generated by the driving system to the thighs, back and shoulders, so as to achieve the effect of lumbar assistance and effectively improve the wearing comfort. There are two active degrees of freedom, which are located at the left and right hips. Each actuator contains of high torque motor and transmission mechanism.

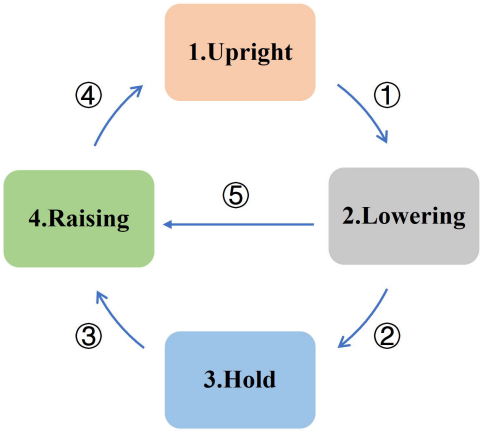

Fig. 2. Finite-State machine of work states of our exoskeleton.

TABLE I
FINITE-STATE MACHINE SWITCH CONDITIONS

Current State	Switching Conditions	Switching Number	Next State
1	$\theta_l \cdot \theta_r < 0, \lvert\theta_l\rvert + \lvert\theta_r\rvert > \theta_{thrL}$	①	2
2	$\lvert\theta_l - \theta_{lmax}\rvert + \lvert\theta_r - \theta_{rmin}\rvert < \theta_{thrR}$	②	3
3	$\lvert\theta_l - \theta_{lmax}\rvert + \lvert\theta_r - \theta_{rmin}\rvert > \theta_{thrR}$	③	4
4	$\lvert\theta_l\rvert + \lvert\theta_r\rvert < \theta_{thrU}$	④	1
2	$\lvert\theta_l - \theta_{lmax}\rvert + \lvert\theta_r - \theta_{rmin}\rvert > \theta_{thrR}$	⑤	4

B. Finite-State Machine

As shown in Fig. 2, four states are defined to describe the work state of this exoskeleton system. (1) Upright state; (2) Lowering state; (3) Hold state; (4) Raising state. In all states, the exoskeleton robot records angle information of the motors. In the Upright state and Lowering state, the motors do not work, which can avoid impeding the user's normal walking; In the Hold state, the motors will maintain their current positions; In the raise state, the motors will track the reference curves to assist the user.

Tab. I describes the finite-state machine switch conditions. θ_l and θ_r are the angle of left motor and right motor, since the two motors are installed symmetrically, when rotating in the same direction, the symbols of the encoders of the two motors are opposite. In this system, when bending forward, the encoder of left motor reads positive and the encoder of right motor reads negative. θ_{thrL} is the threshold of switching lowering, through which the disturbance of some small standing movements can be filtered out. θ_{lmax} and θ_{rmin} are the encoder readings of the left and right motors when the body is at the lowest point, which are kept updated during the lowering state. θ_{thrR} is the threshold of switching raising, which determines the sensitivity of this system.

C. Raising Reference Curve Generator

The raising reference curve is the reference motion curve when the exoskeleton assists, so it is very important. When carrying out the lifting tasks, there must be a lowering action first, so we can utilize people's lowering curve to generate a raising curve. This method is not only more natural, but also in line with user's different habits. Assuming that $s_{down}(t)$ is

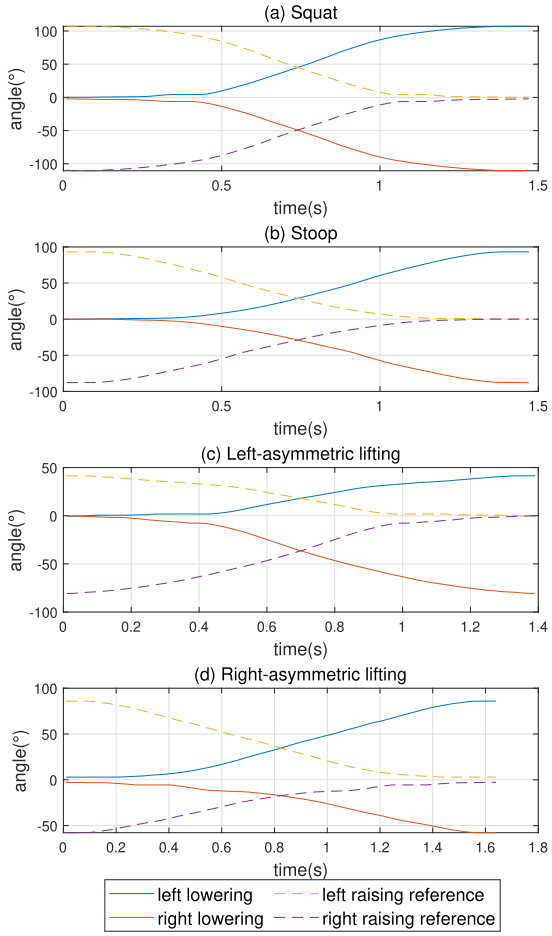

Fig. 3. Lowering curves and generated raising reference assisted curves with various lifting tasks.

the lowering curve recorded during down, t_{total} is the total time spent during down, we define the raising reference curve $y_r(t)$ as:

$$y_r(t) = s_{down}(t_{total} - t), \quad t \in [0, t_{total}] \tag{1}$$

There are lowering curves and generated raising assisted reference curves with mixed lifting tasks by various postures, as shown in Fig. 3. We can see that in squat and stoop, the lowering curves of the two legs are relatively consistent. But, the amplitude of the lowering is somewhat different. In squat, the curve will decline more. However, in left-asymmetric lifting and right-asymmetric lifting, the lowering curves of the two legs are very different, so we cannot utilize the same raising reference curve to assist.

D. System Model

To study the control strategy of the joints, the first problem is to define its dynamic equation. We define the τ_m as the torque of motor, and define θ_e as the rotation angle of motor. During the assistance process, the components of gravity are basically transmitted to the ground through the users' legs, and do not have an impact on the assistance. As shown in Fig. 7, we ignore the gravity, so the simple Lagrange function [20]

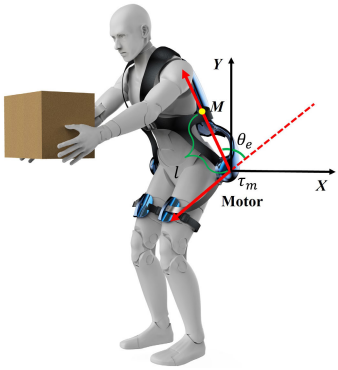

Fig. 4. The simplified system model of the assisted exoskeleton.

of exoskeleton system is:

$$L = \frac{1}{2}M(l\dot{\theta_e})^2,$$
$$\tau_m = \frac{\partial}{\partial t}(\frac{\partial L}{\partial \dot{\theta_e}}) - \frac{\partial L}{\partial \theta_e} \tag{2}$$

where $M = \hat{M}_{body} + \hat{M}_{load} + \hat{M}_{exo}$, $\hat{M}_{body}$, $\hat{M}_{load}$ and $\hat{M}_{exo}$ are the components of the mass of the body, the carrying heavy load and the exoskeleton in the direction of power assistance, so we can get the equation:

$$\ddot{\theta_e} = R\tau_m \tag{3}$$

where $R = 1/Ml^2$. Because the weights of carrying heavy objects are different, and these two components are also changing with the movement of the body, so R is a time-varying parameter, we will use adaptive method to solve it in the control system. During the assistance process, the components of gravity are basically transmitted to the ground through the users' legs, and do not have an impact on the assistance.

E. Development of Adaptive Generalized Predictive Controller

Based on the system model, let $y(t) = \theta_e(t)$, $u(t) = \tau_m(t)$, so we can obtain the transfer function of the system by Laplace transform with zero initial velocity and acceleration:

$$G(s) = \frac{y(s)}{u(s)} = \frac{R}{s^2} \tag{4}$$

So the form of Z transformation is:

$$E(z) = \frac{y(z)}{u(z)} = \frac{RTz}{(z-1)^2} \tag{5}$$

where T is the sampling time, both numerator and denominator are divided by z^2:

$$y(z) = \frac{RTz^{-1}}{1 - 2z^{-1} + z^{-2}}u(z) \tag{6}$$

It can be written in the form of CARIMA model:

$$A(z^{-1})y(k) = B(z^{-1})u(k) + C(z^{-1})\xi(k)/\Delta \tag{7}$$

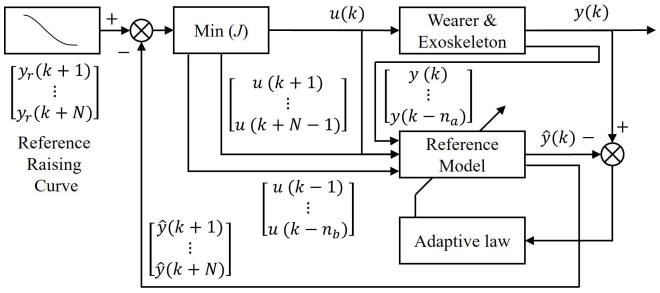

Fig. 5. The overall block diagram of the developed controller.

where $\xi(k)$ is white Gaussian noise, $\Delta = 1 - z^{-1}$ is difference operator, and:

$$\begin{cases} A(z^{-1}) = 1 - 2z^{-1} + z^{-2}, \\ B(z^{-1}) = b_1 z^{-1}, \\ C(z^{-1}) = 1 \end{cases} \tag{8}$$

where $b_1 = RT$, which is the adaptive parameter in this system.

By adding a generalized predictive controller and considering the optimal prediction of step j, the prediction output error at time $k + j$ is:

$$\tilde{y}(k+j|k) = y(k+j) - \hat{y}(k+j|k), \quad j \geq 1 \tag{9}$$

Then, the variance of prediction error is:

$$J = E\{\tilde{y}^2(k+j|k)\} \tag{10}$$

So the minimum $j-step$ optimal predictive control $y^*(k+j|k)$ is given by the following equation:

$$C(z^{-1})y^*(k+j|k) = G_j(z^{-1})y(k) + F_j(z^{-1})\Delta u(k+j-1) \tag{11}$$

where $F_j(z^{-1})$ and $G_j(z^{-1})$ satisfy the following Diophantine equation:

$$\begin{cases} C(z^{-1}) = A(z^{-1})E_j(z^{-1}) + z^{-j}G_j(z^{-1}), \\ F_j(z^{-1}) = B(z^{-1})E_j(z^{-1}). \end{cases} \tag{12}$$

In this system, $C(z^{-1}) = 1$, so the system prediction model can be simplified as:

$$y(k+j) = F_j\Delta u(k+j-1) + G_j y(k) + E_j\xi(k+j) \tag{13}$$

the above equation can be written as a matrix form:

$$\begin{aligned} Y &= F_1\Delta U + F_2\Delta U(k-j) + GY(k) + E\xi \\ &= F_1\Delta U + Y_1 + E\xi \end{aligned} \tag{14}$$

where

$$Y_1 = F_2\Delta U(k-j) + GY(k) \tag{15}$$

Y_1 is the output prediction response based on past inputs and outputs.

$$Y = [y(k+1), y(k+2), \ldots, y(k+N)]^T \tag{16}$$

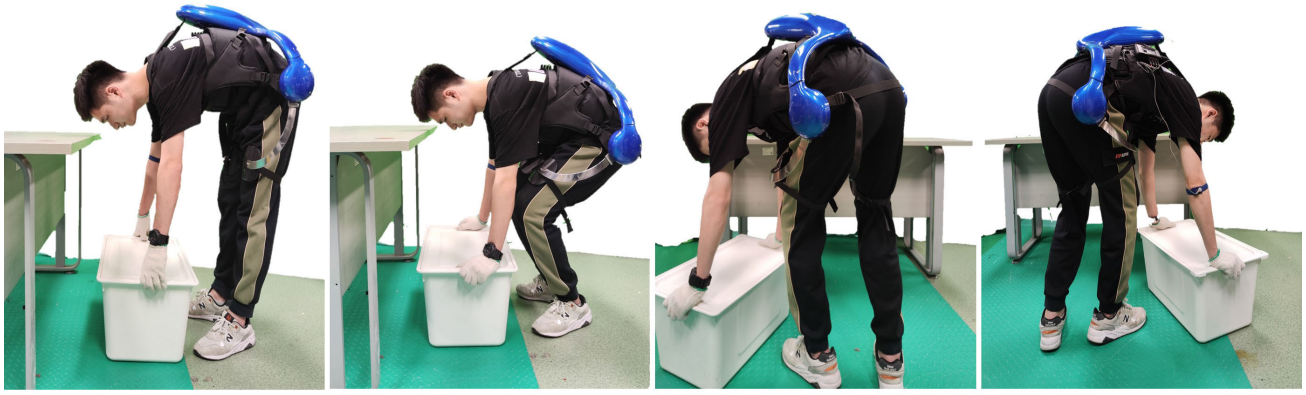

(a) stoop (b) squat (c) left-asymmetric (d) right-asymmetric

Fig. 6. Testers wear exoskeleton and use a variety of postures to complete the lifting tasks.

Y is the future prediction outputs, N is the predicted length.

$$\Delta U = [\Delta u(k), \Delta u(k+1), \ldots, \Delta u(k+N-1)]^T \quad (17)$$

ΔU is the current and future control increment vector.

$$\Delta U(k-j) = [\Delta u(k-1), \Delta u(k-2), \ldots, \Delta u(k-n_b)]^T \quad (18)$$

$\Delta U(k-j)$ is the past control increment vector, n_b is the number of polynomial coefficients in $B(z^{-1})$.

$$Y(k) = [y(k), y(k-1), \ldots, y(k-n_a)]^T \quad (19)$$

$Y(k)$ is the current and past actual outputs, n_a is the number of polynomial coefficients in $A(z^{-1})$.

$$\xi = [\xi(k+1), \xi(k+2), \ldots, \xi(k+N)]^T \quad (20)$$

ξ is the future white noise. So J can be rewritten as:

$$J = E[F_1\Delta U + Y_1 + E\xi - Y_r]^T \times [F_1\Delta U + Y_1 + E\xi - Y_r] + \Delta U^T I \Delta U \quad (21)$$

where Y_r is the future reference output. Let $\frac{\partial J}{\partial \Delta U} = 0$, we can obtain:

$$\Delta U(k) = (F_1^T F_1 + I)^{-1} F_1^T \times [Y_r - F_2\Delta U(k-j) - GY(k)] \quad (22)$$

So the control law $u(k)$ is:

$$\begin{aligned} u(k) &= u(k-1) + \Delta u(k) \\ &= u(k-1) + [1, 0, \ldots, 0](F_1^T F_1 + I)^{-1} F_1^T \\ &\quad \times [Y_r - F_2\Delta U(k-j) - GY(k)] \end{aligned} \quad (23)$$

There are unknown system parameters in this system, so the adaptive algorithm is used to estimate the system parameters online, which can be obtained from equation (7):

$$\begin{aligned} \Delta y(k) &= [1 - A(z^{-1})]\Delta y(k) + B(z^{-1})\Delta u(k-1) + \xi(k) \\ &= \varphi^T(k)\theta + \xi(k) \end{aligned} \quad (24)$$

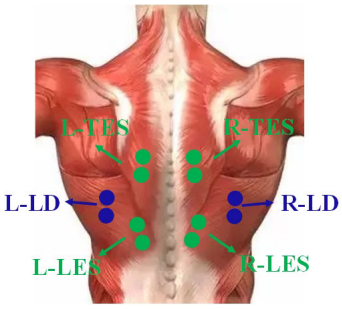

Fig. 7. Measuring electrode position distribution.

where

$$\begin{cases} \varphi(k) = [-\Delta y(k-1), -\Delta y(k-2), \\ \qquad \Delta u(k-1), \Delta u(k-2)]^T \\ \theta = [a_1, a_2, b_0, b_1]^T \end{cases} \quad (25)$$

where a_1, a_2 are coefficients of polynomial $A(z^{-1})$, b_0, b_1 are coefficients of polynomial $B(z^{-1})$.

Using the FFRLS (forgetting factor recursive least squares) algorithm to estimate the system parameters, the following adaptive law can be obtained:

$$\begin{cases} \hat{\theta}(k) = \hat{\theta}(k-1) + K(k)[\Delta y(k) - \varphi^T(k)\hat{\theta}(k-1)], \\ K(k) = \dfrac{P(k-1)\varphi(k)}{\lambda + \varphi^T(k)P(k-1)\varphi(k)}, \\ P(k) = \dfrac{1}{\lambda}[I - K(k)\varphi^T(k)]P(k-1) \end{cases} \quad (26)$$

where λ is the forgetting factor.

At present, the control law and adaptive law of the lumbar assisted exoskeleton are given. We can utilize this controller to help the user complete various lifting tasks.

III. Experiments and Results

A. Participants

In this section, the exoskeleton system is tested by several experiments. There are seven adult males who have no history of spinal disease or lumbar disease volunteer to participate in

this work (age of 26 ± 3 years old, height of 174 ± 6 cm, and weight of 68 ± 8 kg). All of these participants were asked to read experimental protocol and signed an informed consent prior to their participation in the following experiments. This study was approved by the Medical Ethics Committee of Shenzhen Institute of Advanced Technology (SIAT-IRB-200715-H0512, valid time from 2020.01 to 2022.12).

B. Test Produce

Before the experiments, each participant fully understood the test process and was familiar with the operation of the exoskeleton system. In the experiments, participants needed to lift objects of different weights to the table (height: 75cm) with various postures. The object is a box with a size of 60*40*30 cm (length*width*height), and the weights of the objects in the box are 5kg, 10kg and 15kg respectively. As shown in Fig. 6, under each weight, four actions were required to complete the lifting tasks, which are stoop, squat, left-asymmetric and right-asymmetric. Each action was repeated five times, with a 5 minute rest between two actions. First, the subjects completed the above lifting tasks without wearing exoskeleton, and then after half an hour of rest, they wore exoskeleton to repeat the above tasks.

C. Raising Reference Curve Tracking

In the experiments, the predict length N is selected by 8 according our system. We recorded the real-time data of the angles of the exoskeleton. Fig. 8 to Figure 11 show the reference control curves and the actual curves of the exoskeleton when using different postures to carry out lifting tasks. As can be seen from the figures, the maximum errors of the angles are 2.2° and 3.3° respectively at 5kg and 15kg, and all the errors are within 3%. The reference curves are different in the case of different weights and postures, because our control strategy is to plan each person's handling in real time, so as to better adapt to the mixed tasks during handling. The tracking error does not increase in non-sagittal lifting tasks, left handling and right handling, which shows the effectiveness of our control strategy.

D. Assistance Efficiency

The human back has more than 29 muscles involved in weightlifting. Erector spinalis is one of the most important muscles that allow the spine to stand upright. It is located on both sides of the spine and connects the head and tailbone. It is mainly composed of spine and longissimus muscle. Clinical studies have found that most low back pain is caused by spinal muscle strain. Erector spinalis muscle plays a major role in bending and erection. The amplitude of EMG (electromyography) can reflect the activity of muscle, so the erector spinalis muscle is selected as the evaluation index. Erector spinalis muscles includes LD (latissimus dorsi), LES (lumbar erector spinae) and TES (thoracic erector spinae) by one side, so we collected data from six channels. The myoelectric equipment that used to record EMG signals is DataLog MWX8 (Biometrics Ltd.) with sampling rate of 1000 Hz. It has 8 channels and one reference electrode. The small wireless adapter connects to the USB port of a PC host and data input is through a bluetooth communication.

There were three weights in this experiment, which were 5 kg, 10 kg and 15 kg. It was divided into four postures to carry out the lifting task, stoop, squat, left-asymmetric and right-asymmetric, each posture was repeated five times. All tasks were divided into with exoskeleton and without exoskeletons. Therefore, each person got 120 groups of data. There were seven participants in this experiment, so we had a total of 840 groups of data, and each group of data consists of six channels, which were left LD, right LD, left LES, right LES, left TES and right TES. First, the raw data was filtered with a bandwidth of 10-500 Hz. Then, RMS(Root mean square) was calculated for each group of data, and the five groups of data were averaged. The RMS of EMG values of each posture under each weight was obtained. We could get R_E with exoskeleton and R_N without exoskeleton, The assist efficiency of exoskeleton E was obtained from the following formula:

$$E = 1 - \frac{R_E}{R_N} \tag{27}$$

Table II shows statistical test results (all P less than 0.05) of the average RMS of left LD, right LD, left LES, right LES, left TES and right TES for lifting 5 kg, 10kg and 15kg loads respectively by four postures under the two conditions, with and without our exoskeleton. When wearing the waist assisted exoskeleton, the RMS of EMG of the LD, LES and TES are significantly reduced. The average assistance efficiency of exoskeleton are range from 10.52 ± 2.59% to 12.33 ± 3.68 with four postures under lifting 5 kg to 15 kg weight loads. There is no significant change in the assistance efficiency under different postures, which shows that this exoskeleton can effectively assist in a variety of tasks.

Under different loads, the average assistance efficiency are 12.33 ± 3.68%, 11.20 ± 2.95% and 10.52 ± 2.59% under 5 kg, 10 kg and 15 kg loads respectively. With the increase of loads, the assistance efficiency decreases slightly. The assistance effect is basically maintained, and the average assistance effect is more than 10%. This is because our control algorithm adds adaptive parameters, so it can maintain power assistance effect well under different loads.

IV. Discussions

A. Control Strategy

The raising reference curve is the reference motion curve when the exoskeleton assists, so it is very important. This work adopts an innovative method to generate reference raising curve, which utilizes user's lowering curve to generate a raising curve. This is a position control method, compared with the common methods at present, torque control [14] and quintic polynomial position control [19], this method can generate personalized curves according to each lifting task by each person. This way of curves generating enables us to perform a variety of tasks, not only sagittal-plane lifting tasks, which can not be done by other exoskeleton systems, so it can be more suitable for large-scale application in the real working scene.

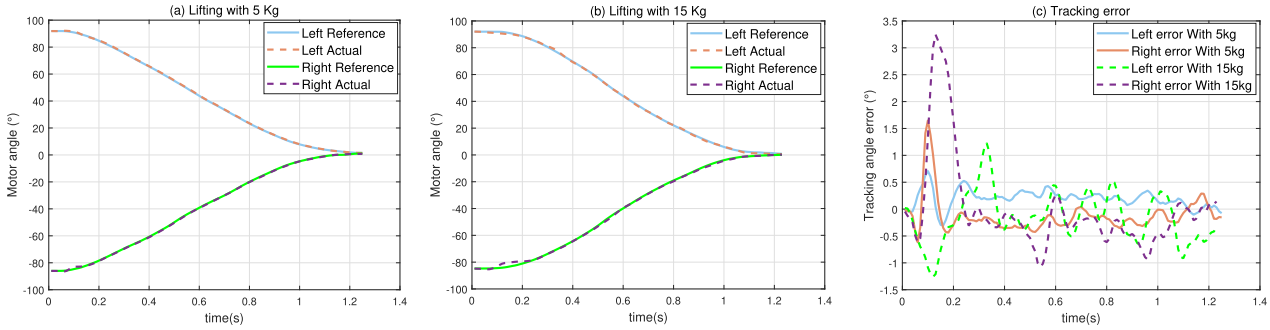

Fig. 8. Tracking results under lifting with stoop. (a) Lifting with 5 kg. (b) Lifting with 15 kg. (c) The tracking errors of lifting with 5 kg and 15 kg.

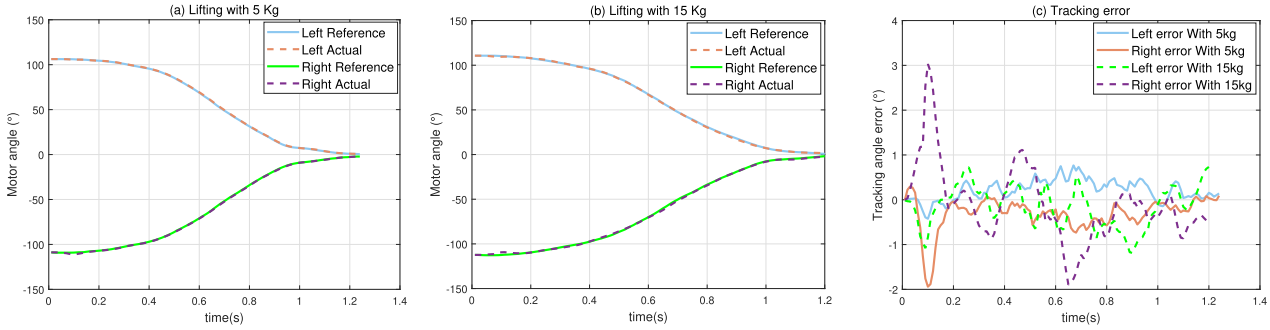

Fig. 9. Tracking results under lifting with squat. (a) Lifting with 5 kg. (b) Lifting with 15 kg. (c) The tracking errors of lifting with 5 kg and 15 kg.

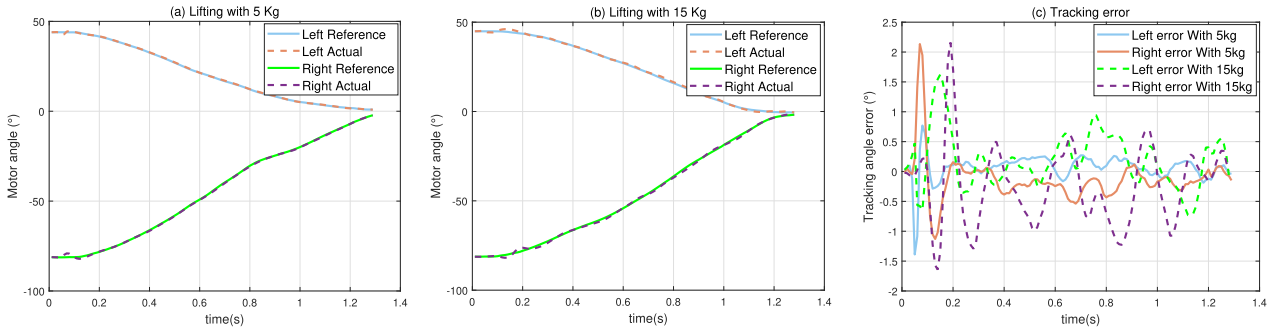

Fig. 10. Tracking results under lifting with left-asymmetric. (a) Lifting with 5 kg. (b) Lifting with 15 kg. (c) The tracking errors of lifting with 5 kg and 15 kg.

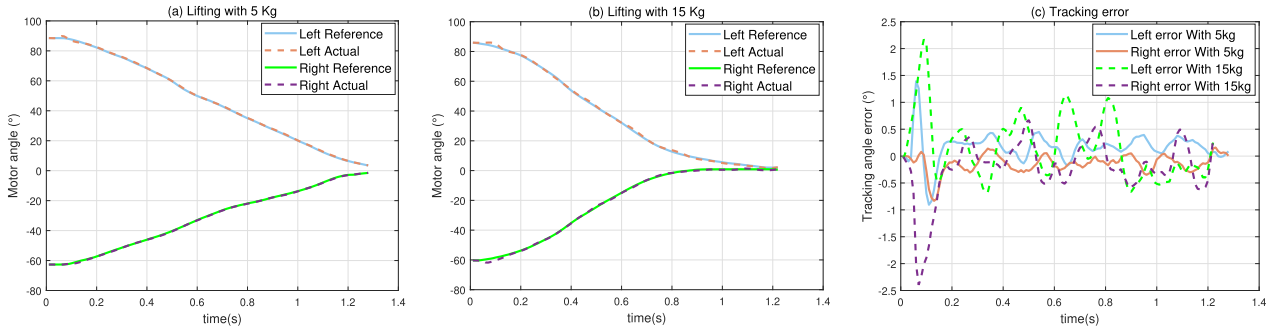

Fig. 11. Tracking results under lifting with right-asymmetric. (a) Lifting with 5 kg. (b) Lifting with 15 kg. (c) The tracking errors of lifting with 5 kg and 15 kg.

It is a natural idea to use predictive control when there is a reference control curve. This work also utilizes the adaptive control law to deal with different lifting tasks and different weights. The experimental results show that the tracking errors of this exoskeleton system are within 3% under four postures and three weights. When the weight changes, the error almost does not change, which shows that our method is effective.

We also investigated seven subjects through the questionnaire, and divided the comfortable level into 1 to 10. We used three different assisted methods, constant torque control,

TABLE II
THE STATISTICAL DATA OF THE ASSISTANCE EFFICIENCY OF EXOSKELETON UNDER DIFFERENT LOADS AND POSTURES

		Assistance Efficiency of Exoskeleton						
Loads	Postures	Left LD (%)	Right LD (%)	Left TES (%)	Right TES (%)	Left LES (%)	Right LES (%)	Mean±SEM
5 kg	Stoop	9.62	12.42	13.22	10.68	12.21	8.16	11.05±1.92
	Squat	12.48	15.15	9.14	7.49	7.87	5.36	9.58±3.60
	Left-asymmetric	10.91	11.72	12.37	12.12	12.57	11.06	11.79±0.69
	Right-asymmetric	15.49	22.02	24.52	12.77	14.48	12.00	16.88±5.16
	Mean±SEM	12.13±2.53	15.33±4.70	14.81±6.71	10.77±2.35	11.78±2.79	9.14±3.01	12.33±3.68
10 kg	Stoop	12.52	15.78	7.50	8.57	9.78	13.40	11.26±3.17
	Squat	5.29	6.02	7.26	5.15	14.41	15.63	8.96±4.77
	Left-asymmetric	8.45	11.93	8.96	7.83	10.37	18.14	10.95±3.82
	Right-asymmetric	10.35	15.30	13.34	12.27	13.84	16.82	13.65±2.27
	Mean±SEM	9.15±3.06	12.26±4.50	9.26±2.82	8.45±2.94	12.10±2.36	16.00±2.01	11.20±2.95
15 kg	Stoop	8.47	8.66	9.92	9.71	8.37	6.88	8.67±1.09
	Squat	8.62	10.28	6.29	13.03	14.91	8.87	10.33±3.15
	Left-asymmetric	9.48	9.68	9.23	12.84	11.07	8.70	10.17±1.53
	Right-asymmetric	12.90	13.43	16.60	10.26	11.16	13.10	12.91±2.19
	Mean±SEM	9.87±2.07	10.51±2.06	10.51±4.35	11.46±1.72	11.38±2.69	9.39±2.63	10.52±2.59

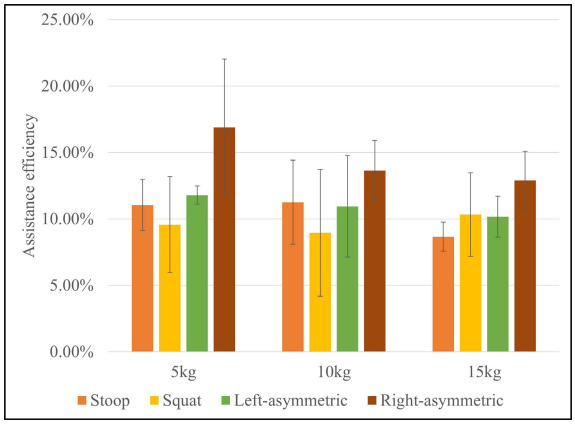

Fig. 12. Average assist efficiency of six channels under different loads and postures.

quintic polynomial position control and the position control of this work. The scores of these three methods were 5.3 ± 0.8, 5.6 ± 0.5 and 6.9 ± 1.1 respectively. It may be because the force received by the subject in torque control is more direct and there is no buffer, so it is the most uncomfortable. The quintic polynomial position control method provides the same curve for everyone under different loads, while our method provides personalized curves according to different people under various tasks, so it is more natural and more comfortable.

B. Evaluation of the Assistance Efficiency

Different with previous lumbar assisted exoskeletons, which can only carry out lifting tasks in the sagittal-plane, our exoskeleton can also assist when completing non-sagittal lifting tasks. As shown in Figure 12, we analyzed the assistance efficiency of exoskeleton in four postures, stoop, squat, left-asymmetric and right-asymmetric under different loads. The average assistance efficiency are 11.79 ± 0.69%, 10.95 ± 3.82% and 10.17 ± 1.53% respectively with left-asymmetric under 5 kg to 15 kg loads, and the average assistance efficiency are 16.88 ± 5.16%, 13.65 ± 2.27% and 12.91 ± 2.19% respectively with right-aysmmetric under 5 kg to 15 kg loads. The average assistance efficiency for six muscles are 10.33 ± 1.44%, 9.62 ± 0.69%, 10.97 ± 0.81% and 14.48 ± 2.11% by lifting loads with stoop, squat, left-asymmetric and right-asymmetric respectively. The average assistance efficiency of left-asymmetric and right-aysmmetric are all higher than 10%. Compared with the stoop and squat, the assistance efficiency do not decrease, and even higher. When executing asymmetrical tasks, workers are required to exert greater force due to the increased range of motion involved, in contrast to symmetrical tasks. As a result, the utilization of exoskeletons can effectively decrease muscle activity in such tasks."Therefore, this exoskeleton can achieve the same assistance effect not only in sagittal-plane lifting tasks, but also in non-sagittal lifting tasks, which shows the effectiveness of our exoskeleton system.

C. Limitations

Although our exoskeleton system performs well in mixed lifting tasks by various postures, this work still has few limitations. Firstly, the assistance efficiency has reached about 10%, but it is still not enough. In the future work, the power of the motors needs to be further increased and the weight of the exoskeleton needs to be reduced. Then, the essence of assisted exoskeleton is to transfer the force from the waist to the supporting thigh when lifting loads, so it may have an impact on the thigh muscles. The future work needs to study the impact of exoskeleton on the thigh muscles and the overall metabolism of the human body.

V. CONCLUSION

In this work, we proposed a new lumbar assisted exoskeleton with mixed lifting tasks by various postures, which can not only complete lifting the tasks of sagittal-plane, but also carry out the lifting tasks of sides. The performance of error tracking and assistance efficiency were comprehensively evaluated. Our novel raising reference curve generator and controller showed good performance. Compared with no exoskeleton, the RMS of EMG were reduced, the effect of exoskeleton robot was verified. For further research, the power of the motors needs to be further increased and the weight of the exoskeleton needs to be reduced. In order to understand the effect of exoskeleton on human body, the impact of exoskeleton on the thigh muscles and the overall metabolism of the human body need to be studied in the future work.

REFERENCES

[1] T. R. Waters, V. Putz-Anderson, A. Garg, and L. J. Fine, "Revised NIOSH equation for the design and evaluation of manual lifting tasks," *Ergonomics*, vol. 36, no. 7, pp. 749–776, Jul. 1993.

[2] T. Kermavnar, A. W. de Vries, M. P. de Looze, and L. W. O'Sullivan, "Effects of industrial back-support exoskeletons on body loading and user experience: An updated systematic review," *Ergonomics*, vol. 64, no. 6, pp. 685–711, 2021.

[3] M. P. de Looze, T. Bosch, F. Krause, K. S. Stadler, and L. O'Sullivan, "Exoskeletons for industrial application and their potential effects on physical work load," *Ergonomics*, vol. 59, no. 5, pp. 671–681, 2016.

[4] Innophys Co. *Muscle Suit*. Accessed: 2023. [Online]. Available: https://innophys.jp/product/

[5] ATOUN. *Atoun Model A*. Accessed: 2022. [Online]. Available: http://atoun.co.jp/products/

[6] M. Gorsic, Y. Song, A. P. Johnson, B. Dai, and D. Novak, "Simultaneously varying back stiffness and trunk compression in a passive trunk exoskeleton during different activities: A pilot study," in *Proc. 43rd Annu. Int. Conf. IEEE Eng. Med. Biol. Soc. (EMBC)*, Nov. 2021, pp. 4886–4890.

[7] W. Wei, W. Wang, Z. Qu, J. Gu, X. Lin, and C. Yue, "The effects of a passive exoskeleton on muscle activity and metabolic cost of energy," *Adv. Robot.*, vol. 34, no. 1, pp. 19–27, Jan. 2020.

[8] M. Gorsic, Y. Regmi, A. P. Johnson, B. Dai, and D. Novak, "A pilot study of varying thoracic and abdominal compression in a reconfigurable trunk exoskeleton during different activities," *IEEE Trans. Biomed. Eng.*, vol. 67, no. 6, pp. 1585–1594, Jun. 2020.

[9] E. P. Lamers and K. E. Zelik, "Design, modeling, and demonstration of a new dual-mode back-assist exosuit with extension mechanism," *Wearable Technol.*, vol. 2, p. e1-26, Jan. 2021.

[10] C. Moon, J. Bae, J. Kwak, and D. Hong, "A lower-back exoskeleton with a four-bar linkage structure for providing extensor moment and lumbar traction force," *IEEE Trans. Neural Syst. Rehabil. Eng.*, vol. 30, pp. 729–737, 2022.

[11] K. Huysamen, M. de Looze, T. Bosch, J. Ortiz, S. Toxiri, and L. W. O'Sullivan, "Assessment of an active industrial exoskeleton to aid dynamic lifting and lowering manual handling tasks," *Appl. Ergonom.*, vol. 68, pp. 125–131, Apr. 2018.

[12] L. Roveda, L. Savani, S. Arlati, T. Dinon, G. Legnani, and L. M. Tosatti, "Design methodology of an active back-support exoskeleton with adaptable backbone-based kinematics," *Int. J. Ind. Ergonom.*, vol. 79, Sep. 2020, Art. no. 102991.

[13] F. Lanotte et al., "Design and characterization of a multi-joint underactuated low-back exoskeleton for lifting tasks," in *Proc. 8th IEEE RAS/EMBS Int. Conf. Biomed. Robot. Biomechatronics (BioRob)*, Nov. 2020, pp. 1146–1151.

[14] T. Poliero, M. Lazzaroni, S. Toxiri, C. Di Natali, D. G. Caldwell, and J. Ortiz, "Applicability of an active back-support exoskeleton to carrying activities," *Frontiers Robot. AI*, vol. 7, p. 157, Dec. 2020.

[15] D. J. Hyun, H. Lim, S. Park, and S. Nam, "Singular wire-driven series elastic actuation with force control for a Waist assistive exoskeleton, H-WEXv2," *IEEE/ASME Trans. Mechatronics*, vol. 25, no. 2, pp. 1026–1035, Apr. 2020.

[16] W. Wei, S. Zha, Y. Xia, J. Gu, and X. Lin, "A hip active assisted exoskeleton that assists the semi-squat lifting," *Appl. Sci.*, vol. 10, no. 7, p. 2424, Apr. 2020.

[17] H.-S. Seong, D.-H. Kim, I. Gaponov, and J.-H. Ryu, "Development of a twisted string actuator-based exoskeleton for hip joint assistance in lifting tasks," in *Proc. IEEE Int. Conf. Robot. Autom. (ICRA)*, May 2020, pp. 761–767.

[18] B. Chen, F. Lanotte, L. Grazi, N. Vitiello, and S. Crea, "Classification of lifting techniques for application of a robotic hip exoskeleton," *Sensors*, vol. 19, no. 4, p. 963, Feb. 2019.

[19] L. Xia, Y. Feng, L. Zheng, C. Wang, and X. Wu, "Development of an adaptive iterative learning controller with sensorless force estimator for the hip-type exoskeleton," in *Proc. IEEE Int. Conf. Robot. Biomimetics (ROBIO)*, Dec. 2019, pp. 2516–2521.

[20] S. B. Niku, *Introduction to Robotics: Analysis, Control, Applications*. Hoboken, NJ, USA: Wiley, 2020.